[CANCER RESEARCH Vol. 6, 3313–3319, June 15, 2000]

New Evidence for an Extra-Hepatic Role of *N*-acetylglucosaminyltransferase III in the Progression of Diethylnitrosamine-induced Liver Tumors in Mice[1]

Xiaoping Yang, Mantu Bhaumik, Riddhi Bhattacharyya, Shih Gong, Charles E. Rogler, and Pamela Stanley[2]

Departments of Cell Biology [X. Y., M. B., R. B., P. S.] and Medicine and Microbiology/Immunology [S. G., C. E. R.], Albert Einstein College of Medicine, New York, New York 10461

ABSTRACT

***N*-acetylglucosaminyltransferase III (GlcNAc-TIII) is encoded by the *Mgat3* gene and catalyzes the addition of the bisecting GlcNAc to the core of *N*-glycans. Mice lacking GlcNAc-TIII due to the insertion mutation $Mgat3^{tm1Pst}$ (termed $Mgat3^{neo}$), exhibit retarded progression of liver tumors induced by diethylnitrosamine (DEN; M. Bhaumik *et al.*, Cancer Res., *58:* 2881–2887, 1998). This phenotype seemed to be due to a reduction, in activity or amount, of a circulating glycoprotein(s) that enhances DEN-induced liver tumor progression. Here, we provide new evidence to support this hypothesis. First, we show that mice with a deletion mutation of the *Mgat3* gene coding exon ($Mgat3^{tmlJxm}$, termed $Mgat3^{\Delta}$) also exhibit retarded progression of DEN-induced liver tumors. At 7 months there was a significant decrease in liver weight (~27%; $P < 0.01$), reflecting reduced tumor burden in $Mgat3^{\Delta/\Delta}$ mice. In addition, tumors were generally fewer and smaller, and histological changes were less severe in $Mgat3^{\Delta/\Delta}$ livers. Therefore, tumor progression is retarded in mice with two different null mutations in the *Mgat3* gene. Second, we show that the development of DEN-induced tumors is unaltered by high levels of GlcNAc-TIII in the liver of transgenic mice. The *Mgat3* gene coding exon under the control of the major urinary protein (MUP) promoter was used to generate transgenic mice that express GlcNAc-TIII in liver. Following DEN injection and phenobarbitol treatment, however, no significant differences were observed between MUP/*Mgat3* transgenic and control mice in either tumor numbers or liver weight. The combined data provide strong evidence that retarded progression of tumors in mice lacking GlcNAc-TIII is due to the absence of the bisecting GlcNAc residue on *N*-glycans of a circulating glycoprotein(s) from a tissue other than liver.**

INTRODUCTION

The glycosyltransferase termed GlcNAc-TIII[3] (E. C. 2.4.144) is encoded by the *Mgat3* gene, which resides on chromosome 15 in mouse (1, 2). GlcNAc-TIII adds the bisecting GlcNAc to complex *N*-glycans (3). The presence of this bisecting GlcNAc residue in complex *N*-glycans increases their affinity for certain lectins, particularly the erythroagglutinin from *Phaseolus vulgaris*, E-PHA (4, 5). At the same time, *N*-glycans with a bisected GlcNAc residue show a reduced affinity for other Gal-binding lectins, particularly ricin (6). These structural effects of the bisecting GlcNAc have functional consequences in cells expressing the *Mgat3* gene. Thus, LEC10 CHO cells, which express GlcNAc-TIII due to a gain-of-function mutation, are ~15 times more resistant to the toxicity of ricin and ~15 times more sensitive to the toxicity of E-PHA than CHO cells (7, 8). Transfection of a *Mgat3* gene causes human hepatoma cells to suppress production of hepatitis B virus (9) and B16 melanoma cells to exhibit reduced experimental metastasis (10). Overexpression of GlcNAc-TIII in PC12 cells perturbs their ability to respond to nerve growth factor (11), and overexpression in a glioma cell line inhibits epidermal growth factor receptor function (12). K562 cells expressing a transfected *Mgat3* gene are comparatively resistant to natural killer cell cytotoxicity and colonize spleen more effectively (13). In mice overexpressing a *Mgat3* transgene in hepatocytes, a reduction in secretion of apolipoprotein and lipids from liver was reported (14). Transgenic mice overexpressing a *Mgat3* transgene in hematopoietic cells were found to have a defect in stroma-dependent hemopoiesis (15).

A role for bisected *N*-glycans in the development of liver cancer was proposed on the basis that GlcNAc-TIII activity increases substantially in tumor tissue following chemical induction of liver tumors in rats (16, 17). Whereas normal rat liver contains almost no detectable GlcNAc-TIII activity and barely detectable GlcNAc-TIII transcripts (18), precancerous hepatic foci have GlcNAc-TIII activity and tumors exhibit a 50–60-fold increase in this activity and contain *Mgat3* gene transcripts that can be detected by northern analysis. These results suggested that hepatic tumors might not occur, or that their development might be significantly reduced, in the absence of GlcNAc-TIII. We previously tested this hypothesis by generating mice homozygous for an insertion mutation that inactivates the *Mgat3* gene ($Mgat3^{tmlPst}$, termed $Mgat3^{neo}$), and subjected $Mgat3^{neo/neo}$ males to DEN-induced hepatocarcinogenesis (19). Compared with wild-type littermates, $Mgat3^{neo/neo}$ males were dramatically retarded in developing liver tumors. At 7 months after DEN injection, mice lacking active GlcNAc-TIII had very few small tumors, whereas wild-type mice had an average of 50 tumors per liver, and their livers weighed twice as much as livers from $Mgat3^{neo/neo}$ mice. However, both DEN-treated $Mgat3^{neo/neo}$ and wild-type mice had similar numbers of precancerous foci, and eventually tumors did develop in $Mgat3^{neo/neo}$ mice. Thus, lack of GlcNAc-TIII did not inhibit the induction phase, but rather it caused a marked retardation in DEN-induced tumor progression.

The $Mgat3^{neo}$ mutant allele gives rise to a read-through transcript that we have shown to be translated into a 371–374 amino acid truncated protein.[4] Although this gene product has no GlcNAc-TIII activity (19), an indirect effect of the protein on tumor progression was a possibility. Therefore, we examined DEN-induced hepatocarcinogenesis in a mutant mouse that lacks GlcNAc-TIII due to deletion of the *Mgat3* gene coding region, a mutation termed $Mgat3^{tmlJxm}$ or $Mgat3^{\Delta}$ (2). Here, we show that DEN-induced tumor formation is also retarded in $Mgat3^{\Delta/\Delta}$ mice. In addition, we show that transgenic mice overexpressing GlcNAc-TIII in liver acquire tumors at essentially the same rate as nontransgenic mice, providing strong evidence for our hypothesis (19) that it is the lack of GlcNAc-TIII on a nonhepatic, circulating glycoprotein(s) that leads to the reduced tumor progression observed in $Mgat3^{-/-}$ mice.

Received 12/20/99; accepted 4/17/00.

The costs of publication of this article were defrayed in part by the payment of page charges. This article must therefore be hereby marked *advertisement* in accordance with 18 U.S.C. Section 1734 solely to indicate this fact.

[1] Supported by National Cancer Institute Grants R37-30645 (to P. S.) and RO1-37232 (to C. E. R.). Partial support was also provided by the Comprehensive Cancer Center at Albert Einstein College of Medicine (Grant PO1-13330).

[2] To whom requests for reprints should be addressed, at Department of Cell Biology, Albert Einstein College of Medicine, 1300 Morris Park Avenue, New York, NY 10461. Phone: (718) 430-3346; Fax: (718) 430-8574; E-mail: stanley@aecom.yu.edu.

[3] The abbreviations used are: GlcNAc-TIII, N-acetylglucosaminyltransferase III; DEN, diethylnitrosamine; MUP, major urinary protein; E-PHA, erythroagglutinin from *Phaseolus vulgaris*; AHF, altered hepatic foci; HCC, hepatocellular carcinoma; PB, phenobarbitol; CHO, Chinese hamster ovary.

[4] R. Bhattacharyya, M. Bhaumik, and P. Stanley, manuscript in preparation.

MATERIALS AND METHODS

Generation of *Mgat3*$^{\Delta/\Delta}$ *Mice.* To derive mice homozygous for the *Mgat3*$^{\Delta}$ (*Mgat3*^{tm1Jxm}) mutation in a genetic background similar to that of mice carrying the *Mgat3*^{neo} (*Mgat3*^{tm1Pst}) mutation examined previously (19), two R1 embryonic stem cell lines, clone 12 and clone 18, that are heterozygous for the *Mgat3*$^{\Delta}$ mutation (2) were kindly provided by Dr. J. D. Marth (University of California, San Diego, CA). These cells were injected into E3.5 C57Bl/6 blastocysts, and chimeras were obtained from both clones, but only chimeras from clone 18 transmitted the mutant allele when crossed with strain CD1 mice (Charles River). First-generation heterozygotes were intercrossed and used in these experiments. The *Mgat3*$^{\Delta}$ allele was detected by PCR or Southern analysis of tail genomic DNA. Primers 184 (sense, AGAGAGGTGATGTGTGATGGG) and 99 (antisense, GAAGATCAGAGGAAGATTCCGC), which flank the targeted *Mgat3* gene coding sequence, were used to detect the *Mgat3*$^{\Delta}$ allele, whereas primers 82 (sense, GCACTAGGCGCAAGTGGGTTGAG) and 83 (antisense, GTAGATGCCCTCGGGTGTGAAG), from within the *Mgat3* gene coding region, were used to identify the endogenous *Mgat3* allele. PCR was carried out through 40 cycles at 94°C for 1 min, 57°C for 1 min, and 72°C for 2 min using Taq polymerase (Perkin-Elmer Corp.). For Southern analysis, genomic DNA (10–20 μg) from liver or tail was digested with *Hind*III (Life Technologies, Inc.), electrophoresed through a 0.8% agarose gel, transferred to Hybond-N nylon membrane (Amersham), and hybridized with probe Y (638 bp; see Fig. 1 in Ref. 19) which is located 434 bp downstream of the *Mgat3* gene coding sequence.

Generation of *MUP/Mgat3* Transgenic Mice. To obtain mice expressing high levels of GlcNAc-TIII in liver, the *Mgat3* gene coding sequence was placed downstream of the MUP promoter in the MUP-SV40-7 vector (20). A *Bam*HI fragment of genomic DNA containing the *Mgat3* gene coding region was treated with Klenow DNA polymerase and dNTPs to obtain blunt ends and inserted into a blunt-ended *Xba*I site, which is located 29 bp downstream of the cap site in the MUP promoter of the MUP/SV40 vector (20). A 5.1-kb *Hin*dIII/*Bam*HI fragment, which contains the MUP promoter, the *Mgat3* gene coding sequence and the SV40 small T intron/poly A signal sequence, was gel purified and injected into fertilized eggs of CBA/B6 mice (F2 generation). Four founders were obtained, and two transmitted the *MUP/Mgat3* transgene after crossing to CD1 mice. However, one was a mosaic, and mice used in this study were derived from founder 19. The *MUP/Mgat3* transgene was identified by PCR and Southern blot analysis of tail DNA digested with *Bgl*II (Boehringer Mannheim). MUP promoter-specific primer 190 (sense, CCAGTTCAGTCTGTACTCCCTC) and *Mgat3* gene-specific primer 192 (antisense, TACCTGGTTTGAAGCACACACC) were used to detect the transgene through 40 cycles of PCR at 94°C for 1 min, 57°C for 1 min, and 72°C for 2 min. Genomic DNA (10–20 μg) was digested with *Bgl*II, hybridized with probe A, which is a 0.46-kb *Pst*I/*Bgl*II fragment within the *Mgat3* gene coding sequence, to determine genotype, transgene integration sites, the number of transgene copies, and the transgene transmission pattern by Southern blot analysis.

Southern Analysis. Genomic DNA (10–20 μg) from tail or liver was digested with either *Bgl*II or *Hin*dIII. After electrophoresis on a 0.8% agarose gel and transfer to nylon membrane, blots were probed with *Mgat3* gene probe A or Y. Rapid hybridization buffer (Amersham) and Prime-it (Stratagene) radioactive labeling kit were used following the manufacturer's instructions. Prehybridization and hybridization were carried out at 65°C for 2 h, respectively. Washing conditions were 0.1× SSC [150 mM sodium chloride and 15 mM sodium citrate (pH 7)], and 0.1% SDS 20 min at room temperature and subsequently 30 min at 65°C.

Northern Analysis. Trizol (Life Technologies, Inc.) was used to extract total RNA from liver, and Oligo (dT) (Pharmacia) was used to purify poly (A)$^+$ RNA from total RNA. Total RNA (20–30 μg) or poly (A)$^+$ RNA (10 μg) was electrophoresed and transferred to nylon membrane. Prehybridization/hybridization buffer contained 50 mM PIPES (piperazine-*N*,*N*′-bis(2-ethanesulfonic acid), 0.1 M NaCl, 50 mM sodium phosphate buffer, 0.5 mM EDTA, 5% SDS, and 60 μg/ml herring sperm DNA. Probe V, a 0.58 kb *Bgl*II/*Pst*I *Mgat3* gene fragment, was used to detect expression of the *Mgat3* transgene and the endogenous *Mgat3* gene. A *Pst*I/*Xho*I 575-bp fragment of the mouse *Mgat1* gene coding region (21) was used to determine integrity and amount of RNA loaded. Prehybridization and hybridization were carried out at 60°C overnight, respectively. Washing conditions were 2× SSC and 0.1% SDS, 20 min at room temperature and subsequently 30 min at 65°C.

Western Blot and E-PHA Blot Analyses. Liver glycoproteins and proteins were extracted with nonionic detergent, and 50-μg aliquots were electrophoresed in a 10% SDS/PAGE gel and transferred to polyvinylidene difluoride membrane, as described previously (19). Desialylation was performed by treatment of the membrane for 1 h at 80°C with 25 mM H_2SO_4. A rabbit polyclonal antibody against amino acids 120–136 of mouse GlcNAc-TIII (TRMLEKPSPGRTEEKTE; synthesized by the Laboratory for Macromolecular Analysis at Albert Einstein College of Medicine, New York, NY) was prepared by Covance Research Products Inc. To purify the antibody, peptide was conjugated to sulfolink coupling gel (Pierce Chemical Co.) to generate an affinity column onto which the serum was applied after blocking the column with 50 mM cysteine. After washing with 10 column volumes of 10 mM HEPES (pH 7.2), the peptide bound antibody was eluted with 0.1 M glycine (pH 2.4) into 0.1 ml of 1 M Tris (pH 8.5), and stored at 4°C in 0.01% thimeresol. Biotinylated erythroagglutinin from *P. vulgaris* (E-PHA; Vector Laboratories Inc.) was used to detect the presence of the bisecting GlcNAc on *N*-glycans, as described previously (19).

Induction of Liver Tumors. DEN (Sigma Chemical Co.) was used to induce hepatoma, as described (19). Briefly, DEN was injected i.p. into male mice at 10 μg/g body weight on day 12 after birth. One month after birth, mice

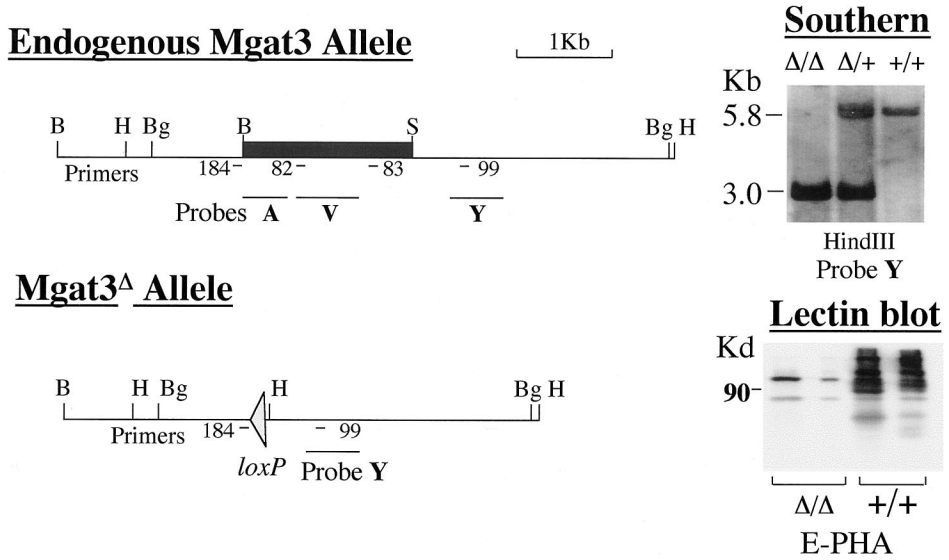

Fig. 1. Characterization of *Mgat3*$^{\Delta/\Delta}$ 129/CD1 mice. The diagram shows the organization of the endogenous *Mgat3* gene coding region and the *Mgat3*$^{\Delta}$ mutant allele with the location of primers and probes used to detect both alleles. A 1.7-kb *Bam*HI/*Sma*I fragment containing the *Mgat3* gene coding sequence was deleted and replaced by a ~160-bp fragment containing a *lox*P site and a *Hin*dIII restriction site to create the *Mgat3*$^{\Delta}$ allele (2). *B, Bam*H1; *Bg, Bgl*II; *H, Hin*dIII; *S, Sma*I. Southern blot analysis: probe Y, 434 bp downstream of *Mgat3* gene coding sequence, was used to distinguish the ~3.0-kb *Mgat3*$^{\Delta}$ allele from the ~5.8-kb *Mgat3*$^{+}$ allele after *Hin*dIII digestion of genomic DNA. Lectin blot analysis: kidney extracts (50-μg protein) were electrophoresed, transferred to membrane, and probed with biotinylated E-PHA, which reacts most strongly with *N*-glycans containing the bisecting GlcNAc.

Table 1 *Hepatocarcinogenesis in Mgat3$^{\Delta/\Delta}$ and Mgat3$^{+/+}$ mice treated with DEN and PB*[a]

	Control (PB)	Control (PB)	P[b]	DEN + PB	DEN + PB	*P[b]
Mgat3 genotype	+/+	Δ/Δ		+/+	Δ/Δ	
Number	5	6		15	15	
Body weight (g)	68.6 ± 7.4	60.9 ± 6.1	0.22	48.5 ± 2.94	51.4 ± 2.65	0.16
Liver weight (g)	3.2 ± 0.2	2.96 ± 0.4	0.34	5.32 ± 0.53	3.88 ± 0.47	**0.007**
Kidney weight (g)	0.8 ± 0.05	0.85 ± 0.05	0.28	0.72 ± 0.03	0.69 ± 0.04	0.26
Tumor no.	0	0		66.1 ± 11.9	53.2 ± 13.3	0.24
Largest tumor (mm)	0	0		10.37 ± 1.85	7.39 ± 1.20	0.10

[a] Data are average ± SE. DEN-treated mice were sibling pairs.
[b] P and *P were calculated by Student's t test and paired t test, respectively.

were given water containing 500 PPM phenobarbitol (Morton Grove Pharmaceuticals, Inc.) until the experiment was terminated.

Analysis of Mice. At different times after DEN injection, mice were weighed, euthanized by injection of 1 ml of 2.5% avertin (tribromomethylalcohol and tertiaryamylalcohol; Aldrich Chemical Co.), and dissected to collect liver, spleen, kidneys, lungs, and blood. Organs were weighed and examined for tumors. Visible tumors were counted, tumor diameter was measured using microcallipers, and each liver was photographed. Slices of liver, kidney, and lung were fixed in 10% formalin, sectioned, and stained with H&E. Remaining liver and kidney tissue was frozen at −80°C. H&E slides containing five liver sections of 5 μm from 22 or 23 mice in each group were scored blindly according to the following numerical criteria based on previously published histological characterization of multistage carcinogenesis in the mouse and rat (22, 23): 0, normal liver; 1, mild, localized dysplasia with mild disruption of hepatic cords, no discernible altered hepatic foci; 2, moderate dysplasia with disruption of hepatic cords, AHF occupy less than 5% of the liver, AHF are approximately 1 mm in diameter; 3, severe dysplasia and disruption of cord structure, predominant AHF prevalent throughout the liver (encompass 20% or more of liver), many exceed 2 mm and appear as distinct nodules on the liver; 4, multiple, large neoplastic nodules present, some of which appear to be early tumors, classified as adenomas when they exceed approximately 4–5 mm; 5, clear HCC present, plus many earlier lesions, HCCs are few in number and rather small, with a predominantly differentiated phenotype; 6, many large HCCs present and some of the tumors have a poorly differentiated phenotype, although differentiated phenotypes are also present.

RESULTS

Retarded Progression of Liver Tumors in Mice with a *Mgat3* Gene Deletion. Mice homozygous for a deletion mutation of the *Mgat3* gene coding exon (*Mgat3*$^{\Delta}$) were generated in a 129/CD1 mixed background, as described in "Materials and Methods." Their genetic background was designed to be as similar as possible to the *Mgat3*$^{neo/neo}$ mice studied previously (19). *Mgat3*$^{\Delta/\Delta}$ mice had the genotype predicted from replacement of the *Mgat3* gene coding exon with a *lox*P sequence (Fig. 1). By PCR, the endogenous *Mgat3* allele was detected as an 0.8-kb product with primer pair 82/83, and the *Mgat3*$^{\Delta}$ allele was detected as an 0.85-kb product with primer pair 184/99 (data not shown). By Southern analysis, the *Mgat3*$^{\Delta}$ allele was identified with probe Y as an ~3-kb *Hin*dIII fragment that reflects the loss of 1.7 kb of the *Mgat3* gene coding sequence and the introduction of ~160 bp containing a *lox*P site and flanking vector DNA. The latter was shown, by sequencing of PCR products, to have introduced a *Hin*dIII site into the targeted locus. The endogenous *Mgat3* allele was identified by a 5.8-kb *Hin*dIII fragment with probe Y (Fig. 1). Also shown in Fig. 1 is a lectin blot of kidney glycoproteins from *Mgat3*$^{\Delta/\Delta}$ and *Mgat3*$^{+/+}$ mice. The lectin E-PHA, which binds bisected *N*-glycans preferentially, did not bind well to glycoproteins from *Mgat3*$^{\Delta/\Delta}$ mice, as expected, if they lack bisected *N*-glycans due to loss of GlcNAc-TIII (2, 19).

Male mice from the second generation of brother:sister matings were injected with DEN at day 12 after birth and given phenobarbitol in their drinking water until 7 months after injection, when they were sacrificed. This regimen replicated our previous experiments in mice homozygous for the *Mgat3*^{neo} insertion mutation (19). At sacrifice, tissues were weighed and prepared for histology. Each liver was photographed, visible tumors on the surface of the liver were counted, and, in several cases, the diameter of all visible tumors was measured. A total of 25 *Mgat3*$^{+/+}$ and 26 *Mgat3*$^{\Delta/\Delta}$ mice were examined. Direct comparison of the two groups revealed that *Mgat3*$^{\Delta/\Delta}$ mice had ~15% less tumors, the size of their largest tumor was smaller (8.1 mm in diameter compared with 10.4 mm), and they had reduced liver weight (19%; $P < 0.04$). These data indicated that tumor progression was retarded in *Mgat3*$^{\Delta/\Delta}$ mice.

To minimize some of the variation due to genetic background, data were compared for the 15 sibling pairs among the cohort of treated mice. It can be seen from Table 1 and Fig. 2 that highly significant differences exist between *Mgat3*$^{+/+}$ and *Mgat3*$^{\Delta/\Delta}$ mice for several parameters. *Mgat3*$^{\Delta/\Delta}$ mice had, on average, fewer tumors than wild-type litter mates (53 compared with 66 per liver), and the average size of their largest tumor was less (7.4 mm compared with 10.4 mm). More significant differences were uncovered when liver weights were compared. The average liver weight of DEN-treated mice was ~27% less for *Mgat3*$^{\Delta/\Delta}$ mice compared with *Mgat3*$^{+/+}$ litter mates ($P < 0.01$; Table 1). When the ratio of liver weight to kidney weight was determined, a reduction of 26% was obtained for *Mgat3*$^{\Delta/\Delta}$ mice ($P = 0.01$; Fig. 2). Similarly, when the ratio of liver to body weight was calculated, Mgat3$^{\Delta/\Delta}$ mice were 32% reduced ($P = 0.01$; Fig. 2). Finally, as expected in mice with a lower tumor burden, *Mgat3*$^{\Delta/\Delta}$ mice were slightly heavier than *Mgat3*$^{+/+}$ mice (Table 1). In control groups, no tumors were obtained and no significant differences were observed in any of these parameters (Table 1).

The gross characteristics of the livers of DEN-treated *Mgat3*$^{\Delta/\Delta}$ and *Mgat3*$^{+/+}$ mice indicated that progression of tumors was significantly slower in *Mgat3*$^{\Delta/\Delta}$ mice. This conclusion was borne out by histological scoring of altered liver morphology, as described in "Materials

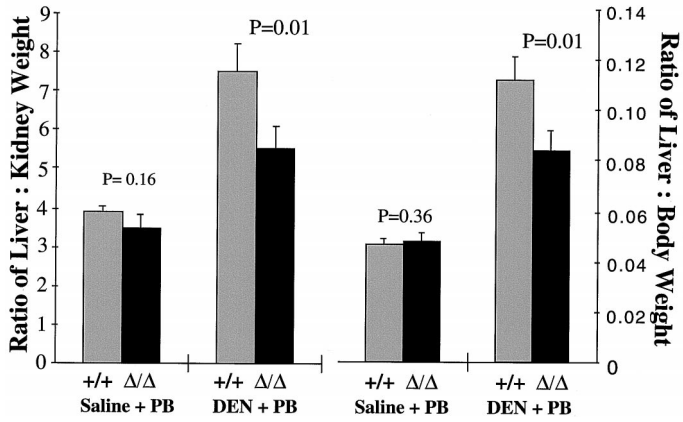

Fig. 2. Liver weight is reduced in *Mgat3*$^{\Delta/\Delta}$ mice. The histogram shows ratios of liver:kidney and of liver:body weight in *Mgat3*$^{\Delta/\Delta}$ and *Mgat3*$^{+/+}$ mice treated with DEN and phenobarbitol (*PB*) or with saline and PB. *Bars*, +SE. *P*s determined by paired Student's t test.

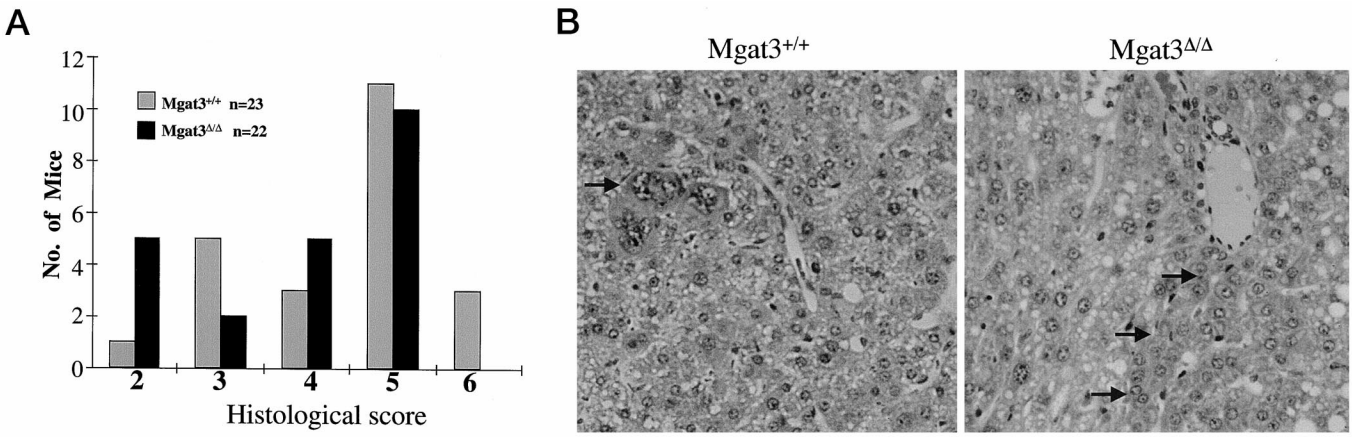

Fig. 3. Histology of liver tumors. *A*, liver sections from mice treated with DEN and PB were stained with H&E, examined by light microscopy in a blinded study, and classified into one of six groups on the basis of transformed liver morphology, as described in "Materials and Methods." A score of 6 reflects the most grossly altered morphology typical of frank hepatocellular carcinoma. *B*, histology of tumors from *Mgat3*$^{+/+}$ and *Mgat3*$^{\Delta/\Delta}$ mice (H&E staining, magnification ×1600). *Left*, a HCC from a *Mgat3*$^{+/+}$ mouse. The *arrow* identifies abnormal nuclei. *Right*, a hepatocellular adenoma from a *Mgat3*$^{\Delta/\Delta}$ mouse revealing a differentiated phenotype. The *arrows* indicate border of adenoma.

and Methods" for categories of 1 (mildly affected) to 6 (most affected). Among the cohort of DEN-treated *Mgat3*$^{\Delta/\Delta}$ mice, not one scored a 6, characteristic of a liver replete with tumors and observed in three *Mgat3*$^{+/+}$ mice (Fig. 3*A*). By contrast, comparatively more DEN-treated *Mgat3*$^{\Delta/\Delta}$ mice scored a 2, characteristic of a liver with few tumor foci and little morphological change (Fig. 3*A*). Histological examination of the tumors in *Mgat3*$^{\Delta/\Delta}$ livers revealed that they were predominantly adenomas with a well differentiated phenotype (Fig. 3*B*). Hepatocytes in these tumors had enlarged nuclei with prominent nucleoli, but highly abnormal nuclei were rare. Some cord-like structure remained in the tumors, further suggesting that the tumors were adenomas rather than carcinomas. In contrast, many of the tumors from wild-type livers had a poorly differentiated phenotype, with pleomorphic nuclei and an acinar or trabecular tumor phenotype, indicative of further progression toward malignancy (Fig. 3*B*).

A reduced level of tumor growth and progression was also evident on examination of gross liver morphology from wild-type and *Mgat3*$^{\Delta/\Delta}$ mice. A picture of a typical *Mgat3*$^{+/+}$ liver that scored 5 by histological classification is shown in Fig. 4*A*. This liver was almost completely replaced by ~150 independent, pale white tumors of varying sizes throughout all lobes of the liver. Histology of this liver revealed very little tissue with a normal cord structure. In contrast, a *Mgat3*$^{\Delta/\Delta}$ liver (Fig. 4*B*) from category 5 did not have as many tumors, and normal cord structure predominated. Thus, even within a category such as 5, *Mgat3*$^{\Delta/\Delta}$ livers were less severely affected. The trend toward less severe tumor formation was also observed in category 2 *Mgat3*$^{\Delta/\Delta}$ livers compared with *Mgat3*$^{+/+}$ livers in category 2 (Fig. 4, *C* and *D*). Tumors were sparse and small in category 2 *Mgat3*$^{\Delta/\Delta}$ livers, consistent with the predominant normal histology of those livers. In contrast, the wild-type liver in this category contained

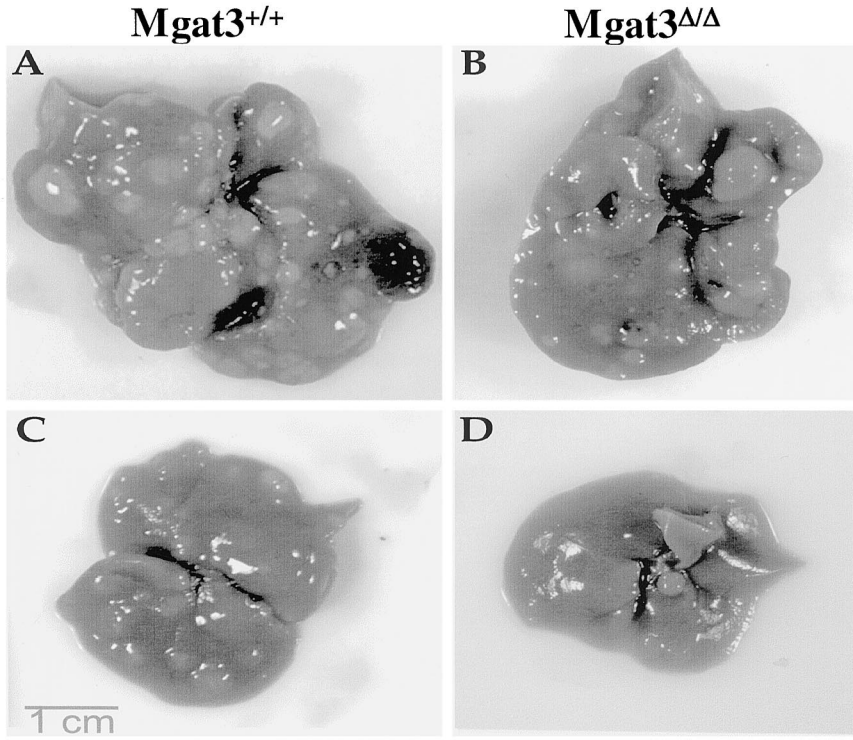

Fig. 4. Gross morphology of livers from *Mgat3*$^{\Delta/\Delta}$ and wild-type mice. Livers from opposite ends of the spectrum of pathologies are pictured. A, *Mgat3*$^{+/+}$ liver, histology classification 5. *B*, *Mgat3*$^{\Delta/\Delta}$ liver, histology level 5. *C*, *Mgat3*$^{+/+}$ liver, histology level 2. *D*, *Mgat3*$^{\Delta/\Delta}$ liver, histology level 2.

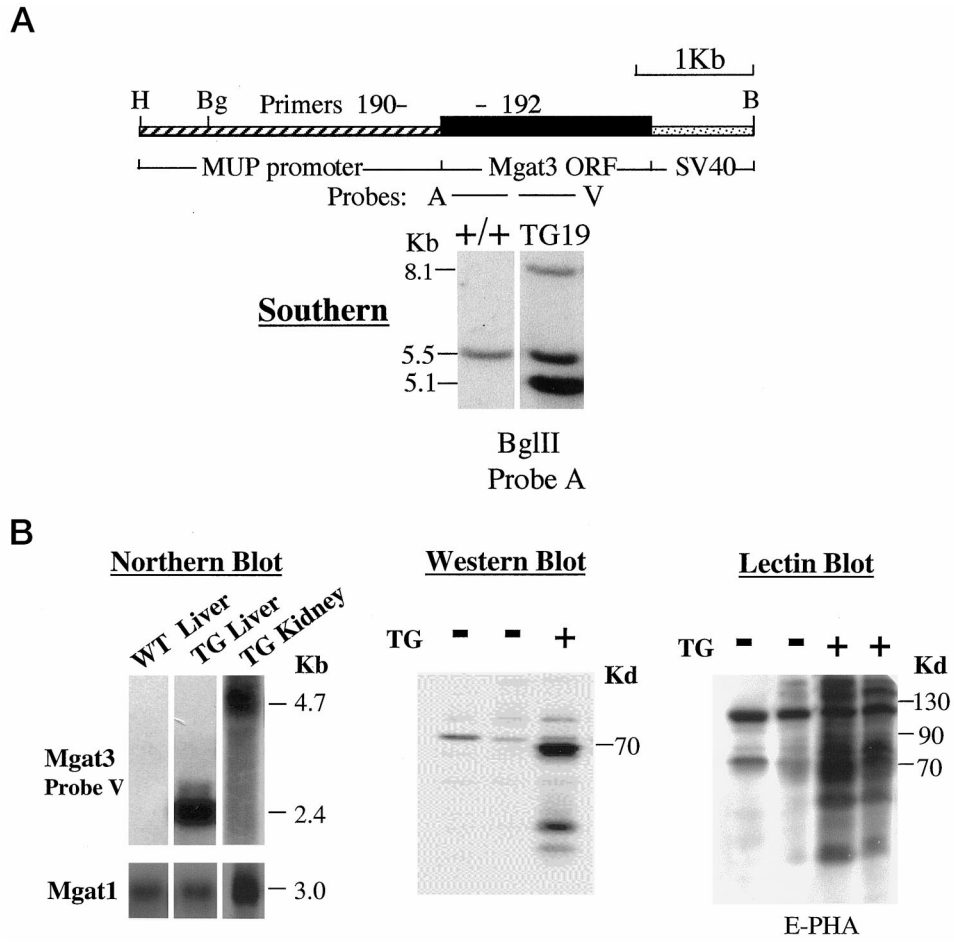

Fig. 5. The *MUP/Mgat3* transgene. Purified linear DNA containing the MUP promoter, a *Bam*H1 fragment of mouse *Mgat3* genomic DNA containing the coding sequence, and the SV40 small T antigen intron and poly(A) addition signal was injected into fertilized eggs to obtain transgenic mice. *Pst*I/*Bgl*I fragment A (0.46 kb) and *Bgl*I/*Pst*I fragment V (0.58 kb) of the *Mgat3* gene coding sequence were used as probes for Southern and northern blot analysis, respectively. MUP promoter-specific primer 190 and *Mgat3* gene-specific primer 192 were used to genotype mice by PCR. *B*, northern analysis: total RNA (~20 μg) from liver was electrophoresed and blotted onto membrane, and *Mgat3* gene transcripts were detected with probe V. Western analysis: liver extracts containing 50 μg of protein were electrophoresed, blotted onto membrane, and probed with an affinity-purified antibody to the NH_2-terminal region of GlcNAc-TIII. A major band at ~70 kD was prominent in transgenic mice (+) and barely detectable in nontransgenic mice (−). Lectin blot analysis: Liver extracts (50-μg protein) were electrophoresed, transferred to membrane, and probed with biotinylated E-PHA. Glycoproteins from transgenic mice (+) bound significantly more E-PHA than glycoproteins from control litter mates (−).

a larger number of tumors. The combined data provide strong evidence that $Mgat3^{\Delta/\Delta}$ mice, lacking GlcNAc-TIII and the ability to add the bisecting GlcNAc to glycoproteins, exhibit reduced progression of liver tumors, as observed previously for mice with the $Mgat3^{neo/neo}$ insertion mutation (19).

Overexpression of a *Mgat3* Transgene in Liver Does Not Significantly Affect the Rate of Tumor Development. Whereas our previous studies showed that the *Mgat3* gene is not up-regulated during hepatocarcinogenesis in mice, *Mgat3* gene transcripts could be detected by reverse-transcription PCR of tumor RNA (19) and might conceivably produce sufficient GlcNAc-TIII to facilitate tumor progression. If the absence of GlcNAc-TIII in liver *per se* is the reason for the reduced progression of tumors in $Mgat3^{-/-}$ mice, overexpression of GlcNAc-TIII in liver should cause DEN-induced tumors to progress faster. To overexpress GlcNAc-TIII in liver, the MUP promoter was used to drive the expression of a *Mgat3* transgene (Fig. 5*A*). The *MUP/Mgat3* transgene was detected by PCR with primer pair 190/192 that gave an 0.8-kb product. For Southern analysis, *Bgl*II digested tail genomic DNA was probed with *Mgat3* gene-specific probe A. Founder 19 and offspring have one integration site with six to seven tandem copies of the *MUP/Mgat3* transgene. Northern analysis showed a strong signal at 2.4 kb from the transgene and did not detect transcripts from the endogenous *Mgat3* gene in liver; western blotting showed that GlcNAc-TIII protein could be readily detected in transgenic but not in nontransgenic mice; and lectin blotting with E-PHA, under conditions optimal for the detection of *N*-glycans with a bisected GlcNAc residue, showed binding to many liver glycoproteins (Fig. 5*B*). Northern analysis of all transgenic mice showed that the *MUP/Mgat3* transgene was highly expressed in the liver of each mouse.

Male transgenic mice from founder 19 and litter mate controls were injected with DEN at 12 days and given phenobarbitol in their drinking water beginning at 1 month after birth. No significant tumors were observed until 5 months in either control or transgenic mice. At that time, tumors were very small and few in number and no differences were apparent between transgenic and nontransgenic mice. A comparison of mice sacrificed from 7–9 months is given in Table 2. Student's *t* test and paired *t* test showed no significant differences between transgenic mice and their nontransgenic litter mates or between transgenic mice and a large group of non-litter mate controls, even for the most sensitive indicator, the ratio of liver to kidney weight (Fig. 6). The gross morphology of tumors and the histological appearance of tumors from the two groups were also indistinguishable. Therefore, increased expression of GlcNAc-TIII in liver does not lead to an earlier appearance of liver tumors nor to an enhanced rate of progression of the tumors induced by DEN.

Table 2 *Hepatocarcinogenesis in MUP/Mgat3 transgenic and nontransgenic mice*[a]

	Transgenic	Nontransgenic	P^b
Tumor number	46.25 ± 8.94	43.29 ± 9.77	0.87
Liver weight (g)	3.77 ± 0.37	4.36 ± 0.36	0.42
Liver:body (ratio)	0.09 ± 0.01	0.099 ± 0.015	0.67
Liver:kidney (ratio)	7.54 ± 0.77	7.46 ± 0.51	0.96
N	24	7	

[a] Data are average ± SE.
[b] Student's *t* test.

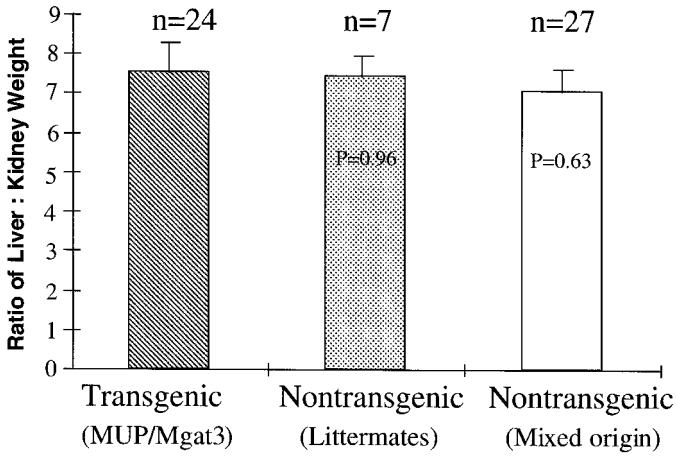

Fig. 6. Liver weights in DEN-treated transgenic and nontransgenic mice. Livers and kidneys of transgenic and nontransgenic litter mates or mice of unrelated origin previously described (19) were weighed at sacrifice 7–9 months after DEN injection. The average ratio of liver:kidney weight was determined. *Bar*, +SE. *P*s were calculated by unpaired Student's *t* test.

DISCUSSION

Previous studies in rats implicated the presence of the bisecting GlcNAc of *N*-glycans in the development of chemically-induced liver tumors (16, 17). Thus, we were not surprised to find that mice lacking GlcNAc-TIII due to an insertion mutation in the *Mgat3* gene got liver tumors much more slowly than wild-type mice (19). However, it was surprising that, in sharp contrast to the situation in rats, the mouse *Mgat3* gene is not induced in liver during hepatocarcinogenesis (Ref. 19 and this study). Thus, we proposed that the mechanism by which GlcNAc-TIII enhances tumor formation is due to an effect of the bisecting GlcNAc on a circulating factor(s) synthesized by a tissue other than liver. Here, we provide new evidence in support of this hypothesis.

First, we have shown that mice with a different *Mgat3* gene-inactivating mutation also exhibit slow growth of DEN-induced tumors (Table 1 and Fig. 2). DEN- and phenobarbitol-treated $Mgat3^{\Delta/\Delta}$ mice had smaller livers, smaller tumors, and less severe histological changes in liver compared with similarly treated $Mgat3^{+/+}$ litter mate controls. For organs such as lung, kidney or spleen, no significant differences were observed between DEN-treated $Mgat3^{\Delta/\Delta}$ and $Mgat3^{+/+}$ mice. These results establish that the development of liver tumors is retarded in $Mgat3^{-/-}$ mice. However, the retardation was significantly less marked in $Mgat3^{\Delta/\Delta}$ mice than the $Mgat3^{neo/neo}$ mice reported previously (19). This could be due to a difference in genetic background since it is well established that responsiveness to DEN varies widely between mouse strains (24–26). $Mgat3^{neo/neo}$ mice contain genetic contributions from the 129SvJ, C57Bl/6, SJL, and CD1 strains, whereas $Mgat3^{\Delta/\Delta}$ mice contain contributions from the two 129 mouse strains that generated R1 ES cells (27) and the CD1 strain used in this study. In fact, differences due to genetic background were apparent because wild-type mice from the two backgrounds given PB in drinking water differed very significantly in body and liver weights, the 129/CD1 mice being significantly heavier, on average, than the mice of more mixed genetic background (Ref. 19 and Table 1). Second, differences could arise between the two $Mgat3^{-/-}$ mutants from the fact that $Mgat3^{neo/neo}$ mice produce a truncated, inactive GlcNAc-TIII from the $Mgat3^{neo}$ allele,[4] whereas the $Mgat3^{\Delta}$ allele produces no product from the *Mgat3* gene coding region. In other experiments, we have found that although the truncated protein does not act as a dominant negative in CHO cell transfectants, it has subtle, neurological phenotypic effects in $Mgat3^{neo/neo}$ (28) and $Mgat3^{\Delta/neo}$ mice.[4]

In a second test of the hypothesis, we investigated whether overexpression of GlcNAc-TIII in liver would enhance tumor formation. The data in Table 2 and Fig. 6 show that mice expressing high levels of GlcNAc-TIII in liver, and nontransgenic control mice that have no detectable expression of the *Mgat3* gene in liver, developed liver tumors at a similar rate that were indistinguishable in appearance. This provides strong evidence that it is not a liver-derived glycoprotein with bisected *N*-glycans that aids DEN-induced tumor progression in mice. Rather, a circulating factor that requires bisected *N*-glycans for optimal activity, or serum half-life, or liver cell binding, or for optimal secretion into the bloodstream is postulated to be missing or reduced in $Mgat3^{-/-}$ mice. Likely tissues that might be a source of a growth factor that stimulates progression of liver tumors are kidney and lung. The *Mgat3* gene is highly expressed in kidney and moderately expressed in lung (1, 2). However, before attempting to correct the $Mgat3^{-/-}$ liver tumor phenotype by other tissue-specific *Mgat3* transgenes, it may be informative to examine the abilities of known glycoprotein growth factors that emanate from kidney or lung to stimulate the growth in culture of hepatocytes from $Mgat3^{+/+}$ and $Mgat3^{-/-}$ mice. Sera from $Mgat3^{+/+}$ and $Mgat3^{-/-}$ mice might also reveal differences in hepatocyte growth stimulatory activities. In addition, it will be of interest to determine the regenerative properties of liver from $Mgat3^{+/+}$ compared with $Mgat3^{-/-}$ mice after partial hepatectomy. If $Mgat3^{-/-}$ livers are slower in regenerating, it may be due to a lack of the same factor that promotes tumor progression.

Acknowledgments

We thank Dr. Thomas Harris for advice and discussions, Melissa Lopez for technical assistance, and Subha Sundaram for purification of antibody.

References

1. Bhaumik, M., Seldin, M. F., and Stanley, P. Cloning and chromosomal mapping of the mouse *Mgat3* gene encoding *N*-acetylglucosaminyltransferase III. Gene, *164:* 295–300, 1995.
2. Priatel, J. J., Sarkar, M., Schachter, H., and Marth, J. D. Isolation, characterization and inactivation of the mouse *Mgat3* gene: the bisecting *N*-acetylglucosamine in asparagine-linked oligosaccharides appears dispensable for viability and reproduction. Glycobiology, *7:* 45–56, 1997.
3. Narasimhan, S. Control of glycoprotein synthesis. UDP-GlcNAc:glycopeptide β4-*N*-acetylglucosaminyltransferase III, an enzyme in hen oviduct which adds GlcNAc in β1–4 linkage to the β-linked mannose of the trimannosyl core of *N*-glycosyl oligosaccharides. J. Biol. Chem., *257:* 10235–10242, 1982.
4. Hammarstrom, S., Hammarstrom, M. L., Sundblad, G., Arnarp, J., and Lonngren, J. Mitogenic leukoagglutinin from *Phaseolus vulgaris* binds to a pentasaccharide unit in *N*-acetyllactosamine-type glycoprotein glycans. Proc. Natl. Acad. Sci. USA, *79:* 1611–1615, 1982.
5. Cummings, R. D., and Kornfeld, S. Characterization of the structural determinants required for the high affinity interaction of asparagine-linked oligosaccharides with immobilized *Phaseolus vulgaris* leukoagglutinating and erythroagglutinating lectins. J. Biol. Chem., *257:* 11230–11234, 1982.
6. Green, E. D., and Baenziger, J. U. Oligosaccharide specificities of *Phaseolus vulgaris* leukoagglutinating and erythroagglutinating phytohemagglutinins. Interactions with *N*-glycanase-released oligosaccharides. J. Biol. Chem., *262:* 12018–12029, 1987.
7. Campbell, C., and Stanley, P. A dominant mutation to ricin resistance in Chinese hamster ovary cells induces UDP-GlcNAc:glycopeptide β-4-*N*-acetylglucosaminyltransferase III activity. J. Biol. Chem., *259:* 13370–13378, 1984.
8. Sallustio, S., and Stanley, P. Novel genetic instability associated with a developmentally regulated glycosyltransferase locus in Chinese hamster ovary cells. Somatic Cell Mol. Genet., *15:* 387–400, 1989.
9. Miyoshi, E., Ihara, Y., Hayashi, N., Fusamoto, H., Kamada, T., and Taniguchi, N. Transfection of *N*-acetylglucosaminyltransferase III gene suppresses expression of hepatitis B virus in a human hepatoma cell line, HB611. J. Biol. Chem., *270:* 28311–28315, 1995.
10. Yoshimura, M., Nishikawa, A., Ihara, Y., Taniguchi, S., and Taniguchi, N. Suppression of lung metastasis of B16 mouse melanoma by *N*-acetylglucosaminyltransferase III gene transfection. Proc. Natl. Acad. Sci. USA, *92:* 8754–8758, 1995.
11. Ihara, Y., Sakamoto, Y., Mihara, M., Shimizu, K., and Taniguchi, N. Overexpression of *N*-acetylglucosaminyltransferase III disrupts the tyrosine phosphorylation of Trk with resultant signaling dysfunction in PC12 cells treated with nerve growth factor. J. Biol. Chem., *272:* 9629–9634, 1997.

12. Rebbaa, A., Yamamoto, H., Saito, T., Meuillet, E., Kim, P., Kersey, D. S., Bremer, E. G., Taniguchi, N., and Moskal, J. R. Gene transfection-mediated overexpression of β1,4-*N*-acetylglucosamine bisecting oligosaccharides in glioma cell line U373 MG inhibits epidermal growth factor receptor function. J. Biol. Chem., *272:* 9275–9279, 1997.
13. Yoshimura, M., Ihara, Y., Ohnishi, A., Ijuhin, N., Nishiura, T., Kanakura, Y., Matsuzawa, Y., and Taniguchi, N. Bisecting *N*-acetylglucosamine on K562 cells suppresses natural killer cytotoxicity and promotes spleen colonization. Cancer Res., *56:* 412–418, 1996.
14. Ihara, Y., Yoshimura, M., Miyoshi, E., Nishikawa, A., Sultan, A. S., Toyosawa, S., Ohnishi, A., Suzuki, M., Yamamura, K., Ijuhin, N., and Taniguchi, N. Ectopic expression of *N*-acetylglucosaminyltransferase III in transgenic hepatocytes disrupts apolipoprotein B secretion and induces aberrant cellular morphology with lipid storage. Proc. Natl. Acad. Sci. USA, *95:* 2526–2530, 1998.
15. Yoshimura, M., Ihara, Y., Nishiura, T., Okajima, Y., Ogawa, M., Yoshida, H., Suzuki, M., Yamamura, K., Kanakura, Y., Matsuzawa, Y., and Taniguchi, N. Bisecting GlcNAc structure is implicated in suppression of stroma-dependent haemopoiesis in transgenic mice expressing *N*-acetylglucosaminyltransferase III. Biochem. J., *331:* 733–742, 1998.
16. Narasimhan, S., Schachter, H., and Rajalakshmi, S. Expression of *N*-acetylglucosaminyltransferase III in hepatic nodules during rat liver carcinogenesis promoted by orotic acid. J. Biol. Chem., *263:* 1273–1281, 1988.
17. Nishikawa, A., Fujii, S., Sugiyama, T., Hayashi, N., and Taniguchi, N. High expression of an *N*-acetylglucosaminyltransferase III in 3′-methyl DAB-induced hepatoma and ascites hepatoma. Biochem. Biophys. Res. Commun., *152:* 107–112, 1988.
18. Miyoshi, E., Nishikawa, A., Ihara, Y., Gu, J., Sugiyama, T., Hayashi, N., Fusamoto, H., Kamada, T., and Taniguchi, N. *N*-acetylglucosaminyltransferase III and V messenger RNA levels in LEC rats during hepatocarcinogenesis. Cancer Res., *53:* 3899–3902, 1993.
19. Bhaumik, M., Harris, T., Sundaram, S., Johnson, L., Guttenplan, J., Rogler, C., and Stanley, P. Progression of hepatic neoplasms is severely retarded in mice lacking the bisecting *N*-acetylglucosamine on *N*-glycans: evidence for a glycoprotein factor that facilitates hepatic tumor progression. Cancer Res., *58:* 2881–2887, 1998.
20. Rogler, C. E., Yang, D., Rossetti, L., Donohoe, J., Alt, E., Chang, C. J., Rosenfeld, R., Neely, K., and Hintz, R. Altered body composition and increased frequency of diverse malignancies in insulin-like growth factor-II transgenic mice. J. Biol. Chem., *269:* 13779–13784, 1994.
21. Yang, J., Bhaumik, M., Liu, Y., and Stanley, P. Regulation of *N*-linked glycosylation. Neuronal cell-specific expression of a 5′ extended transcript from the gene encoding *N*-acetylglucosaminyltransferase I. Glycobiology, *4:* 703–712, 1994 [erratum appears in Glycobiology, *3:* 279, 1995].
22. Frith, C. H., and Ward, J. M. A morphologic classification of proliferative and neoplastic hepatic lesions in mice. J. Environ. Pathol. Toxicol., *3:* 329–351, 1979.
23. Pitot, H. C., and Dragan, Y. P. The multistage nature of chemically induced hepatocarcinogenesis in the rat. Drug Metab. Rev., *26:* 209–220, 1994.
24. Dragani, T. A., Manenti, G., and Della Porta, G. Genetic susceptibility to murine hepatocarcinogenesis is associated with high growth rate of NDEA-initiated hepatocytes. J. Cancer Res. Clin. Oncol., *113:* 223–229, 1987.
25. Vesselinovitch, S. D., Koka, M., Mihailovich, N., and Rao, K. V. Carcinogenicity of diethylnitrosamine in newborn, infant, and adult mice. J. Cancer Res. Clin. Oncol., *108:* 60–65, 1984.
26. Weghorst, C. M., Pereira, M. A., and Klaunig, J. E. Strain differences in hepatic tumor promotion by phenobarbital in diethylnitrosamine- and dimethylnitrosamine-initiated infant male mice. Carcinogenesis, *10:* 1409–1412, 1989.
27. Nagy, A., Rossant, J., Nagy, R., Abramow-Newerly, W., and Roder, J. C. Derivation of completely cell culture-derived mice from early-passage embryonic stem cells. Proc. Natl. Acad. Sci. USA, *90:* 8424–8428, 1993.
28. Bhaumik, M., Sundaram, S., and Stanley, P. Mice lacking GlcNAc-TIII exhibit several biological consequences. Glycobiology, *6:* 720, 1996.